Scientific Journal of Silesian University of Technology. Series Transport
Zeszyty Naukowe Politechniki Śląskiej. Seria Transport

Volume 101 **2018**

p-ISSN: 0209-3324

e-ISSN: 2450-1549

DOI: https://doi.org/10.20858/sjsutst.2018.101.3

Journal homepage: http://sjsutst.polsl.pl

Article citation information:
Brumercik, F., Lukac, M., Majchrak, M., Krzysiak, Z., Krzywonos, L. Teeth geometry and contact pressure calculation of external cycloidal gears. *Scientific Journal of Silesian University of Technology. Series Transport*. 2018, **101**, 27-35. ISSN: 0209-3324. DOI: https://doi.org/10.20858/sjsutst.2018.101.3.

Frantisek BRUMERCIK[1], Michal LUKAC[2], Maros MAJCHRAK[3], Zbigniew KRZYSIAK[4], Leszek KRZYWONOS[5]

TEETH GEOMETRY AND CONTACT PRESSURE CALCULATION OF EXTERNAL CYCLOIDAL GEARS

Summary. Cycloidal (also called epicyclical or convex-concave) gears are used less often than common involute gears, which are very easy to manufacture and can be modified by corrections to the gear profile. Cycloidal gears are very sensitive to the proper axial distance between the pinion and the gear. The main advantage of convex-concave gears is the lowering of the contact pressure due to teeth flanks meshing and also the lowering of the slide ratios compared to involute gears. The calculation of the selected geometrical parameters and the contact pressure between the teeth flanks of the cycloidal gearing is described in the presented article.

Keywords: gear; cycloidal; convex-concave; geometry; contact pressure

[1] Faculty of Mechanical Engineering, University of Zilina, Univerzitna 1 Street, 01026 Zilina, Slovak Republic. Email: brumercikf@fstroj.uniza.sk.
[2] Faculty of Mechanical Engineering, University of Zilina, Univerzitna 1 Street, 01026 Zilina, Slovak Republic. Email: michal.lukac@fstroj.uniza.sk.
[3] Faculty of Mechanical Engineering, University of Zilina, Univerzitna 1 Street, 01026 Zilina, Slovak Republic. Email: maros.majchrak@fstroj.uniza.sk.
[4] Faculty of Production Engineering, University of Life Sciences in Lublin, Akademicka 13, 20-618 Lublin, Poland. Email: zbigniew.krzysiak@up.lublin.pl.
[5] Faculty of Mechanical Engineering, University of Technology, Nadbystrzycka 38 D Street, 20-618 Lublin, Poland. Email: l.krzywonos@pollub.pl.

1. INTRODUCTION

The mathematical model of convex-concave gearing is the basis of the geometry model calculation and as described in detail in [1]. The determination of the geometric parameters in the gear's teeth flanks is based on the equations evaluated from the shape of the path of contact. The general path of contact starting at point A and ending at point E for this type of gearing is presented in Figure 1.

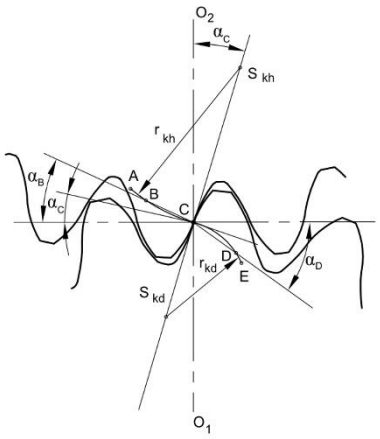

Fig. 1. Path of contact of convex-concave gearing

The arcs of the path of contact are circular arcs defined by their radii r_{kh} for the upper one and r_{kd} for the lower one. The centres of the arcs S_{kh} and S_{kd}, which lie on the common link passing through the contact inflection point C, are defined by the coordinates x_{Skh}, y_{Skh} and x_{Skd}, y_{Skd} in the coordinate system with the origin located in contact point C.

Points A and E are limiting points of the teeth gear mesh. Their position can also be projected onto the teeth flanks' cycloidal curves in both meshing gears, which limits the working area of the teeth flanks [2, 3].

2. GEOMETRY OF THE TEETH FLANKS

The cycloidal teeth can generally be understood as any teeth whose tooth flank forms a curve with a convex and a concave part. Such teeth are present when the contact path is a so-called S-curve, as defined above [4]. Deriving the form of the correctly mating profiles of a cycloidal gearing can be done using basic knowledge of differential geometry and the direct application of the fundamental law of gearing [5]. The main goal of this method is to determine the relation between the pressure angle at various points of the path of contact α and the angle of the gear rotation between pressure angles of two arbitrary points φ_r (α) (Figure 2).

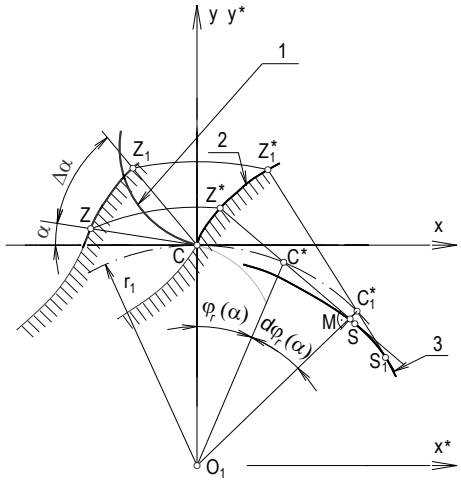

Fig. 2. Relation between the angles α and φ_r:
1) path of contact; 2) tooth flank profile; 3) tooth flank profile evolute

The relation is defined by Equation 1:

$$\varphi_{\mathrm{rh,\,d}} = \pm \frac{2r_{\mathrm{kh,\,d}}}{r_1}\left[\left(\alpha_{\mathrm{h,\,d}} - \alpha_{\mathrm{C}}\right)\cos\alpha_{\mathrm{C}} + \sin\alpha_{\mathrm{C}}\ln\frac{\cos\alpha_{\mathrm{C}}}{\cos\alpha_{\mathrm{h,\,d}}}\right], \tag{1}$$

where:

α - the pressure angle at various points of the path of contact

$\varphi_r(\alpha)$ - the angle of the gear rotation between pressure angles of two arbitrary points and the signs are defined as positive for the upper part and negative for the lower part of the path of contact.

The parametric equations of the gear tooth flank profiles, obtained by the coordinates' transformation of the path of contact's compound of two circular arcs, are defined by the Equation 1.

$$x = \mp 2r_{\mathrm{kh,\,d}}\sin\left(\alpha_{\mathrm{h,\,d}} - \alpha_{\mathrm{C}}\right)\cos\left[\alpha_{\mathrm{h,\,d}} + \varphi_{\mathrm{rh,\,d}}\left(\alpha_{\mathrm{h,\,d}}\right)\right] + r_1\sin\varphi_{\mathrm{rh,\,d}}\left(\alpha_{\mathrm{h,\,d}}\right), \tag{2}$$

$$y = \pm 2r_{\mathrm{kh,\,d}}\sin\left(\alpha_{\mathrm{h,\,d}} - \alpha_{\mathrm{C}}\right)\sin\left[\alpha_{\mathrm{h,\,d}} + \varphi_{\mathrm{rh,\,d}}\left(\alpha_{\mathrm{h,\,d}}\right)\right] + r_1\sin\varphi_{\mathrm{rh,\,d}}\left(\alpha_{\mathrm{h,\,d}}\right). \tag{3}$$

The x and y coordinates are defined for the coordination system with the origin aligned to the point of rotation of the pinion O_1 and the gear O_2. The upper signs in the equations stand for the upper part of the path of contact (indexed with h) and the lower signs in the equations stand for the lower part of the path of contact (indexed with d).

The division of the contact path into an upper and a lower part requires the division of all geometric and other cycloidal gear pair parameters into analogous parts, which will be defined according to the corresponding parts of the contact path curve [6].

It is suitable to derive Equations 2 and 3 into a form that defines the addendum (indexed with a) and the dedendum (indexed with f) of the gear teeth separately.

2.1. Pinion

The coordinates of the pinion 1 addendum flank curve are based on the upper part of the contact path arc dimension, according to the following equations:

$$x_{1a} = -2r_{kh}\sin\left(\alpha_h - \alpha_C\right)\cos\left[\alpha_h + \varphi_{rh}\right] + r_1\sin\varphi_{rh}, \tag{4}$$

$$y_{1a} = +2r_{kh}\sin\left(\alpha_h - \alpha_C\right)\sin\left[\alpha_h + \varphi_{rh}\right] + r_1\cos\varphi_{rh}. \tag{5}$$

The coordinates of the pinion 1 dedendum flank curve is based on the lower part of the contact path arc dimension, according to the following equations:

$$x_{1f} = +2r_{kd}\sin\left(\alpha_d - \alpha_C\right)\cos\left[\alpha_d + \varphi_{rd}\right] + r_1\sin\varphi_{rd}, \tag{6}$$

$$y_{1f} = -2r_{kd}\sin\left(\alpha_d - \alpha_C\right)\sin\left[\alpha_d + \varphi_{rd}\right] + r_1\cos\varphi_{rd}. \tag{7}$$

2.2. External gear

The tooth flank profile coordinates of the external gear 2 can be derived from the equations defined for the pinion 1 considering the gear ratio between them, which is defined as:

$$i_{12} = \frac{\omega_1}{\omega_2} = -\frac{z_2}{z_1} = -\frac{r_2}{r_1}. \tag{8}$$

The coordinates of the external gear addendum flank curve are based on the lower part of the contact path arc dimension, according to the following equations:

$$x_{2a} = +2r_{kd}\sin\left(\alpha_d - \alpha_C\right)\cos\left[\alpha_d + \left(i_{12}\varphi_{rd}\right)\right] + \left(i_{12}r_1\right)\sin\left(i_{12}\varphi_{rd}\right), \tag{9}$$

$$y_{2a} = -2r_{kd}\sin\left(\alpha_d - \alpha_C\right)\sin\left[\alpha_d + \left(i_{12}\varphi_{rd}\right)\right] + \left(i_{12}r_1\right)\cos\left(i_{12}\varphi_{rd}\right) + \left(r_1 + r_2\right). \tag{10}$$

The coordinates of the external gear dedendum flank curve is based on the upper part of the contact path arc dimension, according to the following equations:

$$x_{2f} = -2r_{kh}\sin\left(\alpha_h - \alpha_C\right)\cos\left[\alpha_h + \left(i_{12}\varphi_{rh}\right)\right] + \left(i_{12}r_1\right)\sin\left(i_{12}\varphi_{rh}\right), \tag{11}$$

$$y_{2f} = +2r_{kh}\sin\left(\alpha_h - \alpha_C\right)\sin\left[\alpha_h + \left(i_{12}\varphi_{rh}\right)\right] + \left(i_{12}r_1\right)\cos\left(i_{12}\varphi_{rh}\right) + \left(r_1 + r_2\right). \tag{12}$$

3. SINGLE MESH POINTS

The coordinates of the single mesh points B and D are obtained by solving Equation 1, while considering the angle turns φ_{rAD} and φ_{rEB} to be equal to the angle defined by the pinion tooth pitch [1].

$$\varphi_{rAD} = \varphi_{rAC} + \left|\varphi_{rCD}\right| = \frac{\pi m_t}{r_1}, \tag{13}$$

$$\varphi_{rEB} = \left|\varphi_{rEC}\right| + \varphi_{rCB} = \frac{\pi m_t}{r_1}. \tag{14}$$

The pressure angles α_B and α_D in the single mesh points B and D are calculated using the following transcendental equations:

$$+\frac{2r_{kh}}{r_1}\left[\left(\alpha_A-\alpha_C\right)\cos\alpha_C+\sin\alpha_C\ln\frac{\cos\alpha_C}{\cos\alpha_A}\right]$$
$$+\left|-\frac{2r_{kd}}{r_1}\left[\left(\alpha_D-\alpha_C\right)\cos\alpha_C+\sin\alpha_C\ln\frac{\cos\alpha_C}{\cos\alpha_D}\right]\right|=\frac{\pi m_t}{r_1}, \quad (15)$$
$$\left|-\frac{2r_{kd}}{r_1}\left[\left(\alpha_E-\alpha_C\right)\cos\alpha_C+\sin\alpha_C\ln\frac{\cos\alpha_C}{\cos\alpha_E}\right]\right|$$
$$+\frac{2r_{kh}}{r_1}\left[\left(\alpha_A-\alpha_C\right)\cos\alpha_C+\sin\alpha_C\ln\frac{\cos\alpha_C}{\cos\alpha_A}\right]=\frac{\pi m_t}{r_1}. \quad (16)$$

The single mesh points are important for the definition of the normal force value, which is divided between two pairs of meshing teeth at the path of contact curves AB and CD (Figure 1).

4. CONTACT PRESSURES

The contact pressure calculation is based on Hertz contact theory [3,7], which is also defined for the upper as well as the lower parts of the path of contact by the following equations:

$$p_h=Z_E\sqrt{\frac{F_{1h}}{l\rho_{redh}}}, \quad (17)$$

$$p_d=Z_E\sqrt{\frac{F_{1d}}{l\rho_{redd}}}. \quad (18)$$

The normal forces at the contact points A to C (F_{1h}) and at C to E (F_{1d}) are calculated at the pinion 1, loaded by the input torque M_{k1}, as follows:

$$F_{1h}=\frac{M_{k1}}{r_1\cos\left(\alpha_h\right)} \quad (19)$$

$$F_{1d}=\frac{M_{k1}}{r_1\cos\left(\alpha_d\right)} \quad (20)$$

The reduced Young's modulus of the pinion and gear material is a part of the material coefficient Z_E, which is calculated by Equation 8 [9].

$$Z_E=\sqrt{\frac{1}{\pi\left(\frac{1-\mu_1^2}{E_1}+\frac{1-\mu_2^2}{E_2}\right)}}, \quad (21)$$

where:

$\mu_{1,2}$ - Poisson's ratios of the contact pair materials,

$E_{1,2}$ - Young's moduli of the contact pair materials.

The reduced radius of curvature ρ_{red} is calculated according to these equations:

$$\rho_{redh} = \frac{\rho_{1a}\rho_{2f}}{\rho_{1a} + \rho_{2f}}, \tag{22}$$

$$\rho_{redd} = \frac{\rho_{1f}\rho_{2a}}{\rho_{1f} + \rho_{2a}}. \tag{23}$$

The radii of curvature of the pinion 1 addendum (a) and dedendum (f) are defined as:

$$\rho_{1a} = +2r_{kh}\sin\left(\alpha_h - \alpha_C\right) + \frac{2r_1 r_{kh}\sin\alpha_h\cos\left(\alpha_h - \alpha_C\right)}{2r_{kh}\cos\left(\alpha_h - \alpha_C\right) + r_1\cos\alpha_h}, \tag{24}$$

$$\rho_{1f} = -2r_{kd}\sin\left(\alpha_d - \alpha_C\right) + \frac{2r_1 r_{kd}\sin\alpha_d\cos\left(\alpha_d - \alpha_C\right)}{2r_{kd}\cos\left(\alpha_d - \alpha_C\right) - r_1\cos\alpha_d}. \tag{25}$$

The radii of curvature of the gear 2 addendum and dedendum are defined as:

$$\rho_{2a} = +2r_{kd}\sin\left(\alpha_d - \alpha_C\right) + \frac{2r_2 r_{kd}\sin\alpha_d\cos\left(\alpha_d - \alpha_C\right)}{2r_{kd}\cos\left(\alpha_d - \alpha_C\right) + r_2\cos\alpha_d}, \tag{26}$$

$$\rho_{2f} = -2r_{kh}\sin\left(\alpha_h - \alpha_C\right) + \frac{2r_2 r_{kh}\sin\alpha_h\cos\left(\alpha_h - \alpha_C\right)}{2r_{kh}\cos\left(\alpha_h - \alpha_C\right) - r_2\cos\alpha_h}. \tag{27}$$

5. CALCULATION OF SELECTED GEAR PAIR VALUES

The selected gear pair with the module m = 4 mm and the teeth number z_1 = 16 and z_2 = 24 will represent the application of all derived equations into a model of cycloidal gear pair geometry and the distribution of contact pressure by meshing of the gear teeth.

The geometry is influenced by the module m, the number of teeth z, the radii of the contact path arcs r_{kh} and r_{kd}, and the pressure angle at the point C α_C. The convex-concave condition is satisfied, if there is a valid inequation [1].

$$r_{kh,\,d} < \frac{z_{min} m_n}{4}\cos\alpha_C. \tag{28}$$

The radii of the contact path arcs in the symmetric arrangement within the selected gear pair were defined as $r_{kh} = r_{kd}$ = 8 mm and the pressure angle in the point C as α_C = 20°, which satisfies the inequation (28). The geometry of the selected gear pair is presented in Figure 3.

The contact pressure between the pinion and the gear at the tooth flanks is calculated by the unit values of the torque M_{k1}, the speed w_1 and the gear tooth flank width l, all of which are defined as being equal to 1. The gears are considered from steel with Poisson's ratios $\mu_1 = \mu_2$ = 0.3 and Young's moduli $E_1 = E_2$ = 210000 MPa. The Hertz pressure distribution, as projected onto the pinion and gear teeth flanks, is presented in (Figure 4).

The contact Hertz pressure p_H between the pinion and the gear, up to the angle of the pinion rotation between the pressure angles of two arbitrary points φ_{r1} (α), is shown in Figure 5.

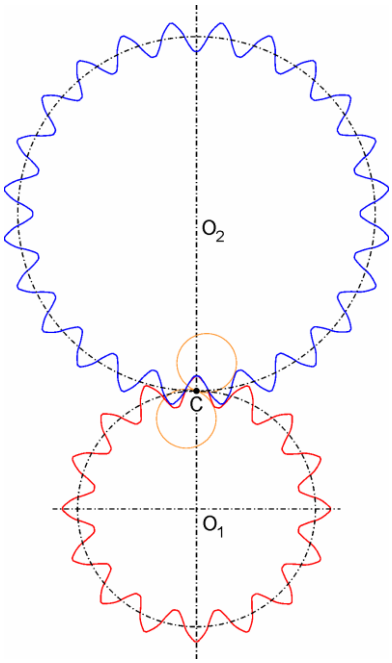

Fig. 3. Geometrical model of the gear pair with cycloidal teeth flanks

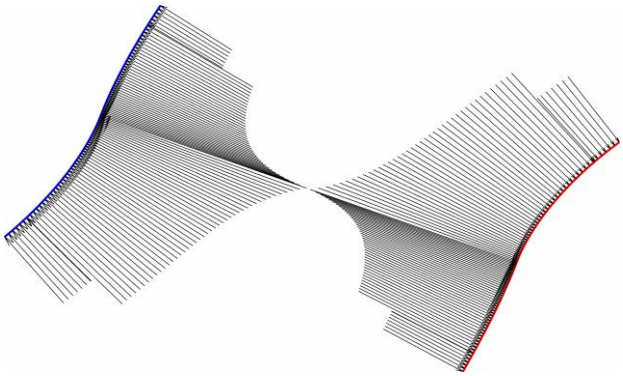

Fig. 4. Hertz pressure distribution projected onto the gear (left) and pinion (right) teeth flanks

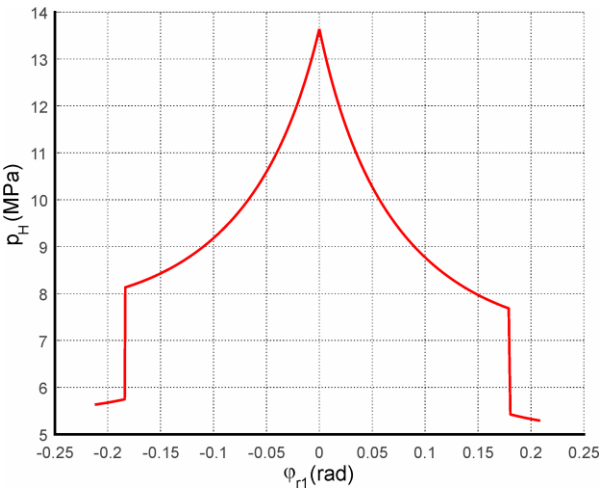

Fig. 5. Hertz's pressure p_H up to angle φ_{r1}

6. CONCLUSION

The article presents a possible approach for modelling cycloidal gear teeth flanks based on the path of contact curves. The calculation of the maximum contact pressure at various points of the gear pair teeth flanks is also defined. The calculation of a selected gear pair is performed by the unit values of the torque, speed and tooth flank width. The obtained model is fully parametric and allows us to calculate the Hertz pressures for various combinations of the characteristic gear pair values, such as the module, the teeth numbers, the pressure angle in the contact point C and the radii of the path of contact curve. The change in the characteristic gear pair values enables us to pursue further research on their influence on Hertz pressure values [9,10,12].

Acknowledgement

The research is supported by the Cultural and Educational Grant Agency of the Ministry of Education, Science, Research and Sport of the Slovak Republic under Project No. 046ŽU-4/2018.

References

1. Veres Miroslav, Miroslav Bosansky, Jan Gadus. 2006. *Theory of convex-concave and plane cylindrical gearing*. Bratislava: Slovak university of technology. ISBN 80-250227-2451-3.
2. Puškár M., M. Fabian, T. Tomko. 2018. „Application of multidimensional statistical model for evaluation of measured data obtained from testing of the HCCI engine prototype". *Diagnostyka* 19(1): 19-24. DOI: http://dx.doi.org/10.29354/diag/78349.
3. Sarkan B., O. Stopka, Ch. Li. 2017. "The issues of measuring the exterior and interior noise of road vehicles". *Komunikacie* 2: 50-55.
4. Glowacz Adam, Zygfryd Glowacz. 2017. „Diagnosis of the three-phase induction motor using thermal imaging". *Infrared physics & technology* 81: 7-16. ISSN 1350-4495. DOI: https://doi.org/10.1016/j.infrared.2016.12.003.
5. Glowacz Adam, Zygfryd Glowacz. 2017. „Diagnosis of stator faults of the single-phase induction motor using acoustic signals". *Applied Acoustic* 117A: 20-27. ISSN 0003-682X. DOI: https://doi.org/10.1016/j.apacoust.2016.10.012.
6. Figlus Tomasz, Mateusz Koziol. 2016. „Diagnosis of early-stage damage to polymer - glass fibre composites using non-contact measurement of vibration signals". *Journal of Mechanical Science and Technology* 30(8): 3567:3576. ISSN 1738-494X. DOI: 10.1007/s12206-016-0717-1.
7. Skrucany Tomas, Branislav Sarkan, Tomasz Figlus, et al. 2017. „Measuring of noise emitted by moving vehicles". *MATEC Web of Conferences* 107: 00072. ISBN: 978-1-5108-4114-7. DOI: https://doi.org/10.1051/matecconf/201710700072
8. Kohar Robert, Slavomir Hrcek. 2014. „Dynamic Analysis of a Rolling Bearing Cage with Respect to the Elastic Properties of the Cage for the Axial and Radial Load Cases". *Communications – Scientific Letters of the University of Zilina* 16 (3A): 74-81. ISSN 1335-4205.

9. Faturik Lukas, Libor Trsko, Slavomir Hrcek, Otakar Bokuvka. 2014. „Comparison of structural design in high and ultra-high cycle fatigue regions". *Transactions of FAMENA* 38 (4): 1-12. ISSN 1333-1124.
10. Nieoczym Aleksander. 2005. „Application of a transportation flux for determining qualitative indices". *Communications – Scientific Letters of the University of Zilina* 7(1): 47-48. ISSN 1333-1124.
11. Figlus Tomasz, Marcin Stańczyk. 2016. "A method for detecting damage to rolling bearings in toothed gears of processing lines". *Metalurgija* 55(1): 75-78. ISSN: 0543-5846.
12. Chepil R., V. Vira, Y. Kharchenko, V. Kulyk, Z. Duriagina. 2018. The peculiarities of fatigue process zone formation of structural materials. *Diagnostyka* 19(4): 27-32. DOI: 10.29354/diag/94754.

Received 05.09.2018; accepted in revised form 20.11.2018